Hindawi
Shock and Vibration
Volume 2021, Article ID 5285494, 14 pages
https://doi.org/10.1155/2021/5285494

Research Article

Vehicle Ride Comfort Analysis Based on Vehicle-Bridge Coupled Vibration

Yichang Zhang,[1] Wusheng Li,[2] Zhe Ji,[1] and Guichun Wang[1]

[1]*School of Civil Engineering, Zhengzhou University, Zhengzhou 450001, Henan Province, China*
[2]*SIPPR Engineering Group Co., Ltd., Zhengzhou 450007, Henan Province, China*

Correspondence should be addressed to Guichun Wang; guichunwang@163.com

Received 16 January 2020; Revised 24 February 2021; Accepted 1 April 2021; Published 15 April 2021

Academic Editor: Mohammad A. Hariri-Ardebili

The study in this paper aims to evaluate the effects of vehicle-bridge coupled vibration on the vehicle ride comfort. The mechanical model of both vehicle and bridge subsystems and the vibration differential equations are established, respectively, based on the principle of dynamic balance and finite element method. The APDL command stream for iterative calculation is compiled on the ANSYS platform. The method to evaluate the vehicle ride comfort is established according to the criteria in ISO2631-1-1997. The vehicle dynamic responses and ride comfort are analyzed considering different pavement levels while multiple vehicles pass through the cable-stayed bridge. The analysis results indicate that the dynamic responses of vehicles decrease with the improvement of pavement roughness, resulting in the vehicle ride comfort to be better; the dynamic responses of vehicles increase with the increment of vehicle speed or the decrement of vehicle gravity, resulting in the vehicle ride comfort to be worse. The present research results can provide an insight into the rational design of bridge structure so as to reduce the vehicle-bridge coupling vibration responses and improve the ride quality of drivers and passengers.

1. Introduction

When vehicles pass through a long-span bridge, the dynamic interaction between vehicles and bridge often occurs due to the roughness of road surface. This phenomenon is called vehicle-bridge coupling vibration and is usually affected by vehicle running parameters. The research on this subject includes the analysis of dynamic responses of bridge structure, running stability, and vehicle ride comfort.

The main difficulty is that the interaction between the two subsystems cannot be determined by a simple method. Therefore, it is necessary to establish the dynamic model and the dynamic interaction model of vehicles and bridge. The road roughness needs to be described mathematically, and the vibration differential equations of the system should be established. The solution to the problem should be obtained by numerical method [1–4].

The structure of the paper is arranged as follows. The concepts of vehicle-bridge coupling vibration and vehicle ride comfort are introduced in the first part. In the second part, the available achievements are summarized, leading to the main content of this paper. In the third part, the analysis method is introduced, including establishing the model of vehicle-bridge coupling vibration, the differential equations of vehicle-bridge system and solution, and the vehicle comfort analysis method. In the fourth part, the influences of the roughness of the bridge deck, vehicle speed, and weight on vehicle comfort are analyzed. In the fifth part, the implication of the study is discussed. In the last part, the research conclusions are summarized. The article flowchart is shown in Figure 1.

2. Literature Review

The analysis on dynamic responses of vehicle-bridge coupling vibration has gone through the process from analytical method to numerical method and has achieved fruitful research results [5–8]. Simplifying the bridge structure into a simply supported Euler-Bernoulli beam, Wu and Law simulated the moving force into a Gaussian random process and proposed a random analysis method for the dynamic interaction between vehicle and bridge [9]. Provornaya and Glushkov recommended three

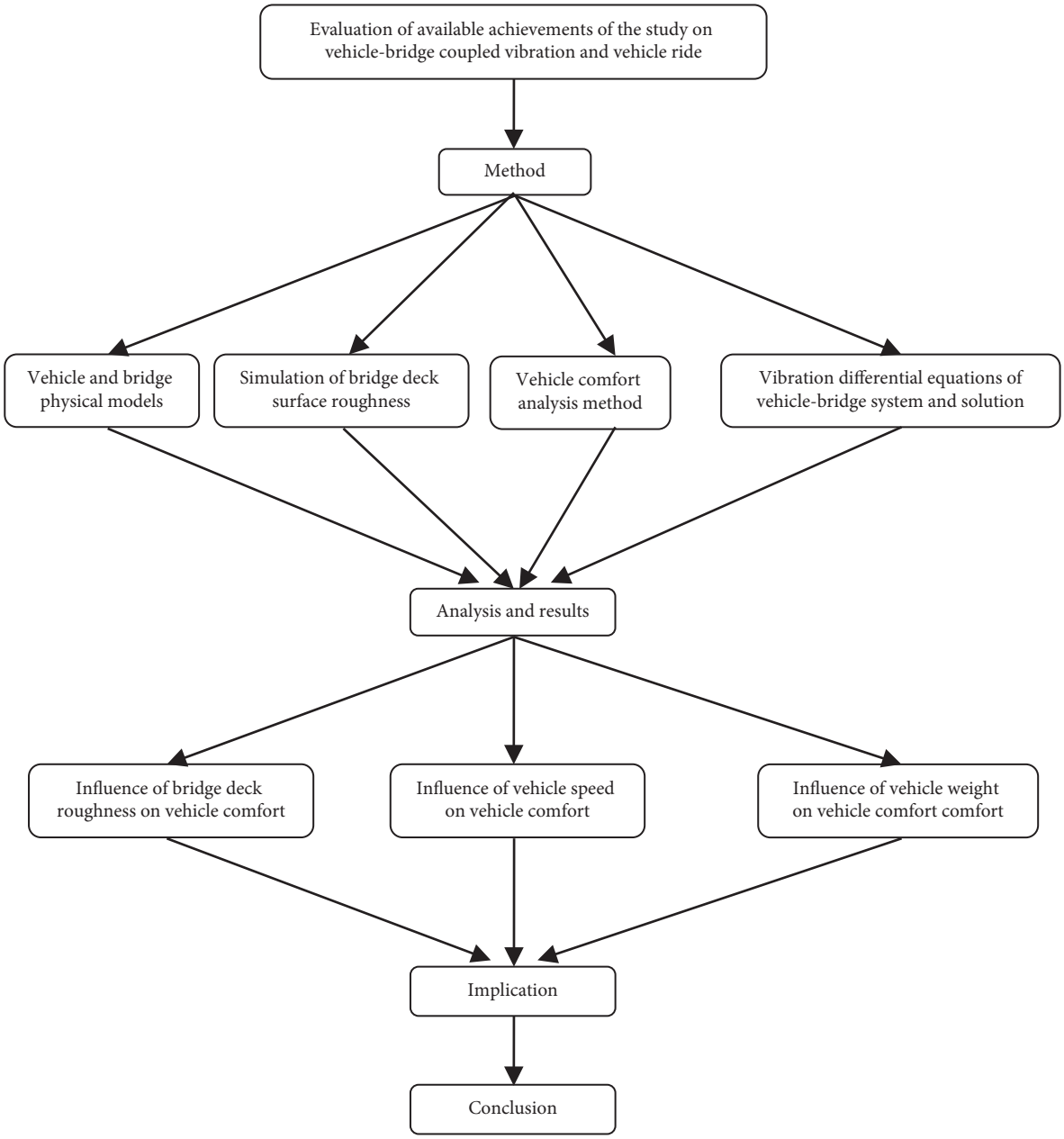

Figure 1: Article flowchart.

different simplified models to study the vibration of the bridge due to running vehicles and calculated the bridge responses by numerical method [10]. Ouchenane studied the influence of multiple moving load fleets on the dynamic responses of the bridge and compared it with the analysis results of the CSI bridge. It is found that the displacement of the bridge increases with the increment of the load of the fleet, and the dynamic magnification factor of the medium velocity is obtained. Ignoring that the parameters of the unidimensional model do not affect the results, the structural dynamic magnification of the unidimensional model and the three-dimensional model is almost the same [11].

The above researches focused on the dynamic responses of bridge structure; however, they did not discuss the vehicle dynamic responses and vehicle comfort. Vehicle ride comfort refers to the discomfort degree felt by drivers and conductors during vehicle running. The action of the coupling vibration of the vehicle-bridge may intensify the vibration of the vehicle and even cause the vehicle to jump and move significantly, resulting in violent lateral sway, pitch rotation, and large lateral movement. Although the coupling vibration of most vehicle-bridge systems cannot lead to an obvious threat to the safety of bridge structure and the vehicles, however, the vibration of vehicle-bridge systems may be very strong and the vehicle ride comfort is very poor from the perspective of drivers and conductors. Particularly for the vehicles running at high speed on long-span bridges, the problem of ride comfort probably becomes more serious.

The continuous improvement of people's living standards inevitably leads to higher and higher requirements for vehicle ride comfort.

It has become an important item in bridge engineering design to consider the influence of vehicle-bridge coupling vibration on vehicle ride comfort [12–14]. In recent years, the research on this subject has made some progress and obtained some achievements.

Hu and Wang took simply supported beams as examples to analyze the vertical acceleration of vehicles based on vehicle-bridge coupling vibration and to evaluate the influence of vehicle-bridge coupling vibration on vehicle ride comfort [15]. Taking into account the influence of wind load, Xu and Guo used a numerical method to analyze the influence of road roughness and vehicle and bridge parameters on vehicle ride comfort [16]. Taking Hangzhou bay bridge as an example and considering the road roughness and dynamic characteristics of the vehicle-bridge system, Han and Chen set up a wind-vehicle-bridge dynamic interaction model and analyzed the vehicle comfort based on the coupling vibration of vehicle-bridge [17, 18]. Zhang et al. analyzed the comfort of railway vehicles when they pass through the bridge by numerical method [19]. Wu et al. studied the influence of pavement deck curing warping on vehicle ride comfort [20]. Gao et al. proposed a dynamic analysis method to solve train-beam interaction based on the frequency domain and evaluated the train vibrations by a ride comfort index based on weighted third-octave acceleration magnitudes [21].

The above researches focused on a single vehicle model and mainly considered the influence of vertical acceleration and roll acceleration on vehicle ride comfort. The vehicle comfort problem of the vehicle-bridge coupling vibration system is very complicated and involves many factors [22–24]. In addition, some new long-span bridges continuously appear, many problems need to be further studied [25]. In this paper, a new numerical method was established to analyze the vehicle dynamic responses and vehicle ride comfort based on the vehicle-bridge coupling vibration. Fujian Changmen highway cable-stayed bridge with a span of 550 m was taken as the background, and in the analysis on vehicle ride comfort, the influence of vehicle vertical, pitching, and rolling vibration accelerations was considered according to the method proposed by ISO2361-1997 [26].

3. Methods

3.1. Analysis Model of Vehicle-Bridge Coupling Vibration

3.1.1. Three-Dimensional Finite Element Model of Changmen Bridge. Fujian Changmen bridge is a long-span bridge crossing the Minjiang River on the Fuzhou city beltway, which locates in downstream of the Minjiang River. The main bridge is a cable-stayed bridge with composite beam, two towers, double cable planes, and the spans of $41.9 + 49.6 + 57.5 + 550 + 64.5 + 60.5 = 824$ m. The middle span main girder adopts a closed flat streamline steel box girder and the side span main girder is reinforced concrete single box four-chamber box girder. The main tower is vase-shaped and made of C50 concrete. When establishing the finite element model, the cable adopts Link10, only the tension is considered, the damping is set as 0.02, and the stress-strain intersection system is calculated with the equivalent elastic modulus method. The cable is fixedly connected with the bridge tower. The bridge tower adopts BEAM4, the box girder adopts BEAM188, and the simplified transverse stiffening beam also adopts BEAM4. The length of each beam element is 1 meter. The mass of the bridge deck is reduced to the beam. The finite element model of a cable-stayed bridge with 537 nodes and 970 elements is built on the ANSYS platform. The schematic diagram of the finite element model of the bridge is shown in Figure 2. The bridge deck with a width of 33.5 m has six lanes in both directions. The layout of vehicles on the bridge deck is shown in Figure 3.

3.1.2. Vehicle Model. The vehicle is modeled in three dimensions, with front and rear wheels on separate beams and left and right wheels on the same beam. As shown in Figure 4, the vehicle model includes 9 degrees of freedom; they are the vertical displacements $z_1 \sim z_6$ of six wheels, the vertical displacement z_v, pitch angle displacement θ_v, and the lateral inclination displacement φ_v of the vehicle body. The symbol m_v is the mass of the vehicle body; $m_1 \sim m_6$ are, respectively, the mass of six wheels (including vehicle suspension frame mass); $k_{u1} \sim k_{u6}$ and $c_{u1} \sim c_{u6}$ are, respectively, vehicle suspension stiffness and damping; $k_{d1} \sim k_{d6}$ and $c_{d1} \sim c_{d6}$ are, respectively, the tire stiffness and damping. Specific parameters are set as follows: $m_1 = m_2 = 335$ kg, $m_3 \sim m_6 = 670$ kg, $m_v = 24990$ kg, $k_{u1} = k_{u2} = 71.805$ kN/m, $k_{u3} \sim k_{u6} = 165.159$ kN/m, $c_{u1} \sim c_{u6} = 240572$ kg/s, $k_{d1} = k_{d2} = 26.796$ kN/m, $k_{d3} \sim k_{d6} = 48.091$ kN/m, and $c_{d1} \sim c_{d6} = 2340$ kg/s. The pitch moment of inertia and roll moment of inertia of the vehicle body are 6140 kg·m² and 3201 kg·m².

3.1.3. Mathematical Simulation of Bridge Deck Surface Roughness. There are several methods to simulate the roughness of bridge pavement, among which the trigonometric series method is widely used because of its strict theoretical foundation and stable and reliable algorithm. In this paper, the road roughness is simulated by the trigonometric series method as a stationary Gaussian random process with ergodic states, as described by

$$r(x) = \sum_{k=1}^{N} a_k \cos(\omega_k x + \phi_k), \tag{1}$$

where x is the distance from an irregularity point on bridge surface to the initial point of the bridge; $r(x)$ is the irregularity value at the irregularity point; a_k is the road power spectral density, $a_k = \sqrt{4G_d(n_k)\Delta n}, G_d(n_k); n_k$ is spatial frequency,
$n_k = n_l + (k - (1/2))\Delta n, k = 1, 2, \ldots, N; \Delta n = (n_h - n_l)/N$,
and n_h and n_l are upper and lower limits of spatial frequency. The circular frequency $\omega_k = 2\pi n_k$ and ϕ_k is the phase angle.

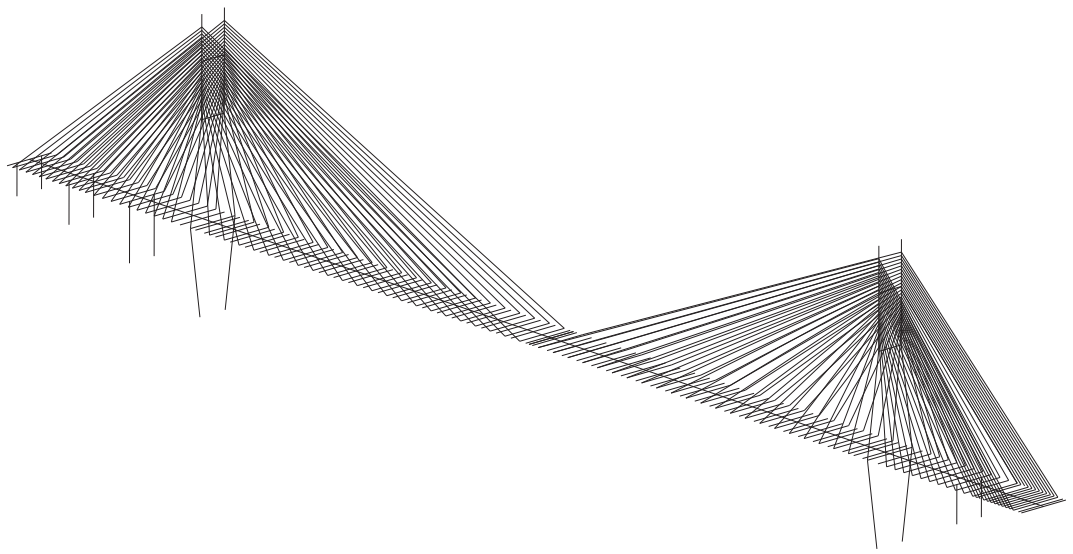

Figure 2: Bridge finite element model.

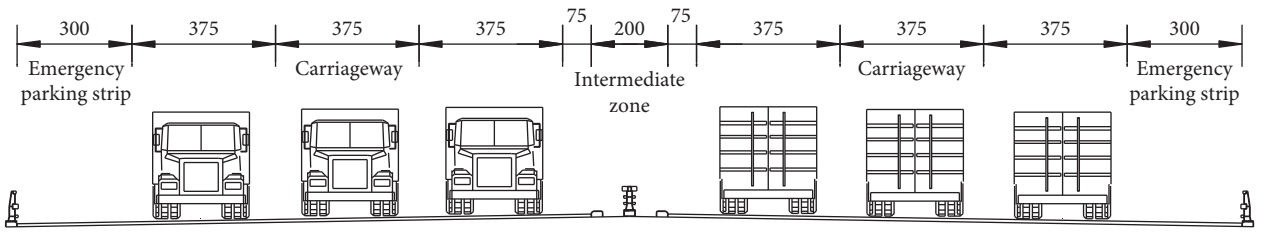

Figure 3: Layout of vehicles on bridge deck (unit: cm).

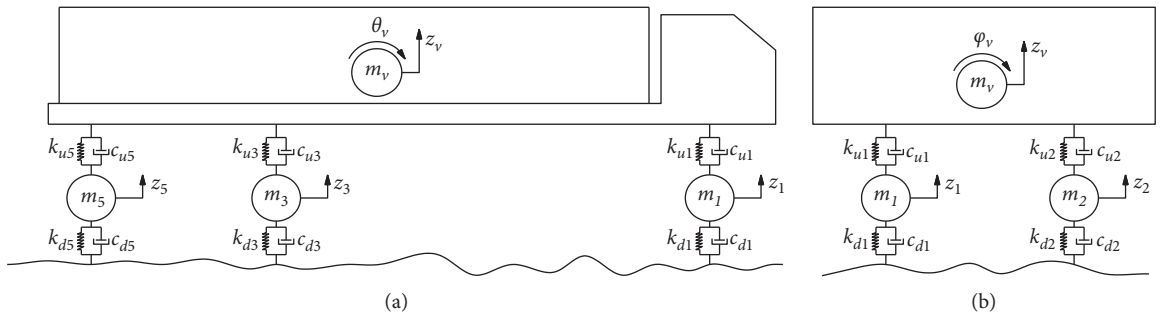

Figure 4: Vehicle model. (a) Elevation. (b) Side view.

China national standard GB7031 divides the road into eight levels. According to the actual situation of the road in China, the first four levels are selected to simulate the roughness of the road surface. Figure 5 shows the sample function of roughness on the road of level B, which is calculated by the numerical analysis software MATLAB.

Figure 6 shows the curve of the peak roughness on the road surface at different road levels changing with the level of road. Among them, the peak roughness values on the road of level B, C, and D are, respectively, 2.00, 4.01, and 8.04 times that on the road of level A, which increase approximately by geometric series.

Using the model established in this paper, the dynamic responses of the structure are calculated, and the results are

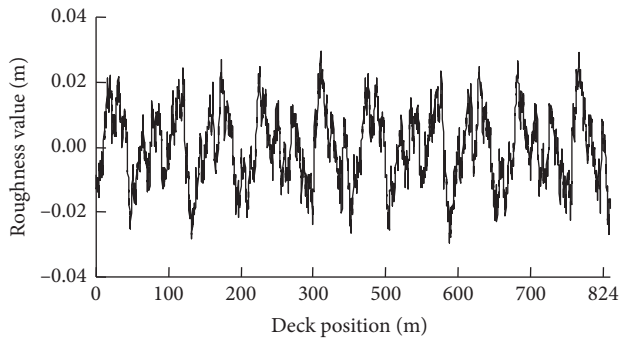

Figure 5: Sample function of roughness on the road of level B.

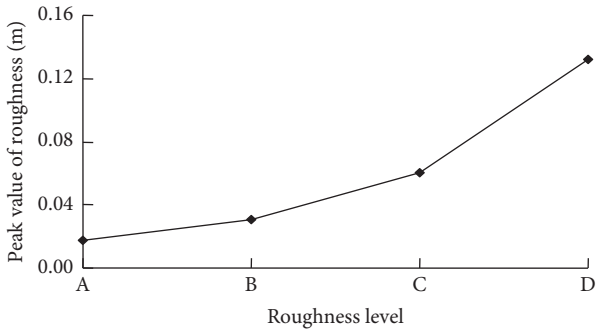

Figure 6: The variation curve of peak values of road roughness for various levels.

compared with the available research results. It is found that the dynamic displacement, acceleration, internal force, and cable stress of the main beam conform to the basic laws of vehicle-bridge coupling vibration. The process and results of dynamic analysis of bridge structure verify the validity and correctness of the model established in this paper, which can be applied to vehicle comfort analysis based on vehicle-bridge coupling vibration.

3.2. The Establishment of and Solution to Vibration Differential Equation of the Vehicle-Bridge System

3.2.1. Differential Equation of Vibration. After the mechanical model of the vehicle-bridge system is established, its vibration differential equation should also be established and solved by coupling the two subsystems with the coordinate conditions of force and displacement. The matrix form of the vehicle vibration differential equation can be written as

$$\mathbf{M}_v\ddot{u}_v\ (t) + \mathbf{C}_v\dot{u}_v(t) + \mathbf{K}_v\mathbf{u}_v(t) = \mathbf{F}_v(t), \tag{2}$$

where $\mathbf{M}_v$, $\mathbf{C}_v$, and $\mathbf{K}_v$ are generalized mass, damping, and stiffness matrices of vehicles and $\mathbf{u}_v(t)$, $\dot{u}_v(t)$, $\ddot{u}_v(t)$, and $\mathbf{F}_v(t)$ are, respectively, vehicle displacement, velocity, acceleration, and load vectors. The matrix form of the vibration differential equation of the bridge structure can be written as

$$\mathbf{M}_b\ddot{Z}_b\ (t) + \mathbf{C}_b\dot{Z}_b(t) + \mathbf{K}_b\mathbf{Z}_b(t) = \mathbf{P}_b(t), \tag{3}$$

where $\mathbf{M}_b$, $\mathbf{C}_b$, and $\mathbf{K}_b$ are, respectively, mass, damping, and stiffness matrices of the bridge structure and $\mathbf{Z}_b(t)$, $\dot{Z}_b(t)$, $\ddot{Z}_b(t)$, and $\mathbf{P}_b(t)$ are, respectively, displacement, velocity, acceleration, and equivalent nodal load vectors of the bridge structure.

The dynamic interaction between vehicle and bridge is influenced by the displacement and force at the contact points between wheels and bridge. In the analysis of vehicle-bridge coupling vibration, the following assumptions are made according to the interactive effects:

① The tires are always in contact with the deck, and $\Delta\mathbf{Z}(t)$ is the relative value of the vertical displacement vector of bridge to wheel group. $\Delta\mathbf{Z}(t)$ can be defined by

$$\Delta\mathbf{Z}(t) = \mathbf{Z}_b(t) - \mathbf{Z}_v(t) + \mathbf{r}(x), \tag{4}$$

where $\mathbf{Z}_b(t)$ is the vertical displacement vector of the bridge at the contact point; $\mathbf{Z}_v(t)$ is the vertical displacement vector of the wheel at the contact point with the road surface, and its elements include $z_1 \sim z_6$; $\mathbf{r}(x)$ is the road roughness value vector of the contact point.

② The force acting on the contact surface of the tire and the bridge adheres to the D'Alembert principle; that is, the dynamic interactive force between vehicle and bridge is equal in magnitude and opposite in direction. It can be described as

$$\mathbf{P}_b(t) = -\mathbf{P}_v(t) = \mathbf{C}_d\Delta\dot{Z}(t) + \mathbf{K}_d\Delta\mathbf{Z}(t), \tag{5}$$

where $\mathbf{P}_b(t)$ is the force vector that vehicles exert on the bridge; $\mathbf{P}_v(t)$ is the force vector that bridge applies to vehicle; they are action and reaction. $\mathbf{C}_d$ and $\mathbf{K}_d$ are, respectively, the damping and stiffness matrices of the wheel group; $\Delta\dot{Z}(t)$ is the vertical relative velocity vector of bridge to wheel group.

3.2.2. Solution to Vibration Differential Equation and Convergence Criterion. At present, the piecewise analytic method, central difference method, Newmark-β method, and Wilson-θ method are more commonly used in the time domain stepwise integration method. Considering the convergence, stability, accuracy, and efficiency of the algorithm, we use the Newmark-β method to solve the differential equation of the vehicle-bridge coupling vibration system.

The key points to solve the vibration differential equation of bridge structure with the Newmark-β method are illustrated in the following. For convenience, the subscript b of the vector and matrix is omitted.

① The equivalent nodal load vector of bridge structural vibration system at time $t + \Delta t$ can be written as

$$\overline{P}_{t+\Delta t} = \mathbf{P}_{t+\Delta t} + \mathbf{M}\left(a_0\mathbf{Z}_t + a_2\dot{Z}_t + a_3\ddot{Z}_t\right) + \mathbf{C}\left(a_1\mathbf{Z}_t + a_4\dot{Z}_t + a_5\ddot{Z}_t\right), \tag{6}$$

where $\overline{P}_{t+\Delta t}$ is the equivalent node load vector at time $t + \Delta t$; $\mathbf{P}_{t+\Delta t}$ is the node load vector at time $t + \Delta t$; $\mathbf{M}$ and $\mathbf{C}$ are, respectively, the mass and stiffness matrices of the structure. $\mathbf{Z}_t$, $\dot{Z}_t$, and $\ddot{Z}_t$ are, respectively, the displacement, velocity, and acceleration vectors of the bridge structure at time t; $a_0 \sim a_5$ are the integral parameters.

② The displacement at time $t + \Delta t$ is solved by

$$\overline{K}\mathbf{Z}_{t+\Delta t} = \overline{P}_{t+\Delta t}, \tag{7}$$

where $\overline{K}$ is the equivalent stiffness matrix of the structure, which is related to the mass, stiffness, and damping distribution of the structure; $\mathbf{Z}_{t+\Delta t}$ is the

displacement vector at time $t + \Delta t$; $\overline{P}_{t+\Delta t}$ is the same as above.

③ Acceleration and velocity vectors of structure at time $t + \Delta t$ can be calculated by

$$\ddot{Z}_{t+\Delta t} = a_0 \left(\mathbf{Z}_{t+\Delta t} - \mathbf{Z}_t\right) - a_2 \dot{Z}_t - a_3 \ddot{Z}_t, \tag{8}$$

$$\dot{Z}_{t+\Delta t} = \dot{Z}_t + a_6 Z_t + a_7 Z_{t+\Delta t}, \tag{9}$$

where a_6 and a_7 are integral parameters.

Thus, given the initial conditions of vehicle and bridge (including mass, stiffness, damping, displacement, and acceleration), the solution to the vehicle-bridge coupling vibration differential equation can be obtained. Using parametric design language APDL, we compiled the command stream on the platform of ANSYS to solve the vehicle-bridge coupling vibration differential equation iteratively.

In this paper, displacement tolerance is used to control the convergence of the calculation process; it can be described as

$$\frac{\left\|\mathbf{Z}^i - \mathbf{Z}^{i-1}\right\|}{\left\|\mathbf{Z}^i\right\|} \le \varepsilon, \tag{10}$$

where $\mathbf{Z}^{i-1}$ and $\mathbf{Z}^i$ are, respectively, the displacement vectors at contact points of vehicle and bridge calculated during the $i-1$th and ith iterations. $\|\mathbf{Z}^i\|$ is the norm of $\mathbf{Z}^i$; ε is the control parameter of displacement. On the basis of comprehensive consideration of calculation time cost and result accuracy, referring to other relevant literature and summing up experiences in calculation practice, the displacement convergence control parameter ε is set as 0.01 in this paper.

3.3. Vehicle Comfort Analysis Method. The comfort analysis method is closely related to vehicle speed. The main evaluation methods of vehicle comfort include absorption power method, ISO2631 method, comprehensive evaluation method, and IRI method. Lprencipe et al. [27, 28] showed that ISO2631 is suitable for the evaluation of the comfort of low speed; this paper studies the speed in 5 m/s~40 m/s, and the speed is relatively low. Therefore, this paper uses the ISO2631 method to evaluate vehicle comfort.

ISO2631-1-1997 method takes the sitting human body under vibration as the analysis model. As shown in Figure 7, the driver and passenger lean on the seat, and the vehicle vibration is transmitted to the human body through the seat supporting surface, the foot supporting surface, and the seatback.

In the analysis, the following 12 degrees of freedom were considered:

① Center point of seat support surface: the line displacements of vibration x_s, y_s, and z_s in the three axial directions at hip and the vibration angle displacements r_x, r_y, and r_z around the three axes.

② Center point of seatback: three axial vibration line displacements of back x_b, y_b, and z_b.

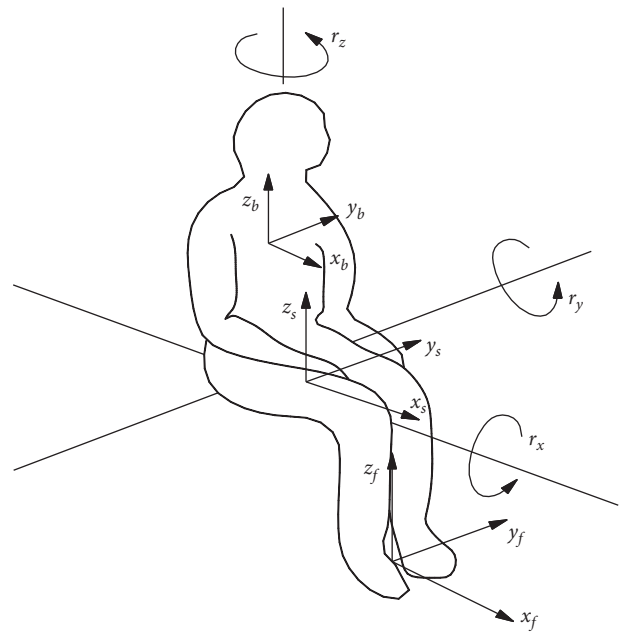

Figure 7: The coordinate system of sitting human body.

③ Center point of the foot support surface: three axial vibration line displacements x_f, y_f, and z_f at sole of foot.

This method takes the total weighted acceleration RMS (root mean square) and weighted vibration level as evaluation indexes. The relationship between them and comfort level is listed in Table 1. The total weighted acceleration RMS is calculated by the following:

$$a_v = \left[\sum_{i=1}^{N} \left(k_i a_{\omega i}\right)^2\right]^{1/2}, \tag{11}$$

where N is the number of degrees of freedom. k_i is the weighted coefficient of vibration acceleration RMS. $a_{\omega i}$ is the acceleration RMS of the ith degree of freedom.

As the vehicle vibrations affecting comfort are mainly composed of the vertical vibration, lateral vibration, and pitch vibration of the vehicle body, equation (11) can be simplified as

$$a_v = \left[\left(k_1 a_{\omega 1}\right)^2 + \left(k_2 a_{\omega 2}\right)^2 + \left(k_3 a_{\omega 3}\right)^2\right]^{(1/2)}, \tag{12}$$

where $k_1 = 1$ m/s; $k_2 = 0.4$ m/rad; $k_3 = 0.63$ m/rad. They are, respectively, the weighted coefficients of vertical, pitch, and lateral vibration acceleration RMSs; $a_{\omega 1}$, $a_{\omega 2}$, and $a_{\omega 3}$ are, respectively, the vertical, pitching, and rolling vibrations acceleration RMSs of the vehicle body; their units are, respectively, m/s^2, rad/s^2, and rad/s^2. The level of weighted vibration can be calculated by the following formula:

$$L_{\text{eq}} = 20 \lg\left(\frac{a_v}{a_0}\right), \tag{13}$$

where a_0 is the reference acceleration RMS, $a_0 = 10^{-6}$ m/s^2.

Table 1: The relationship among the ride comfort level, weighted vibration level, and total weighted acceleration RMS value.

Weighted vibration level L_{eq} (dB)	Total values of the weighted RMS acceleration a_v (m/s^2)	Reactions
< 110	< 0.315	Not uncomfortable
110~116	0.315~0.63	A bit uncomfortable
114 ~120	0.5~1	Somewhat uncomfortable
118~124	0.8~1.6	Uncomfortable
122~128	1.25~2.5	Very uncomfortable
> 126	> 2.0	Extremely uncomfortable

4. Analysis and Results

In the following calculation, if not specified, the level of road roughness is B; the spacing of vehicles is (50 ± 5) m; the speed of vehicles is 20 m/s; the weight of the vehicle is 30 t. The vehicles are arranged at six lanes of two ways, with a fleet lining at each lane, and the traffic flow is continuous.

4.1. Influence of Bridge Deck Roughness on Vehicle Comfort

4.1.1. Analysis of Vibration Acceleration of Vehicle Body. The time-history curves of vertical, pitching, and rolling vibration accelerations for the cases with bridge deck roughness of levels A and D are, respectively, shown in Figures 8–10. The amplitudes of vertical, pitching, and rolling accelerations for the case with bridge deck roughness of level D are much larger than those for the case with bridge deck roughness of level A.

The variation curves of peak accelerations of vertical, pitching, and rolling vibrations with the different levels of bridge surface irregularity are shown in Figures 11–13. It can be seen that, with the deterioration of the bridge surface irregularity, the peak accelerations of the vertical, pitching, and rolling vibrations gradually increase. For the case with bridge deck roughness of level A, the peak accelerations of vertical, pitching, and rolling vibrations of the vehicle body are the smallest and are, respectively, 1.32 m/s^2, 1.26 rad/s^2, and 3.60 rad/s^2. For the case with bridge deck roughness of level D, they are the largest and are, respectively, 9.80 m/s^2, 9.71 rad/s^2, and 23.13 rad/s^2, being increased by 6.42, 6.71, and 5.43 times. Therefore, the irregularity of the bridge deck has a significant impact on the vibration of the vehicle body but also seriously affects the comfort of vehicles.

4.1.2. Vehicle Ride Comfort Analysis. The variation curve of weighted vibration acceleration RMS value with the change of bridge deck irregularity level is shown in Figure 14. As can be seen from Figure 14, with the deterioration of bridge deck condition, the weighted vibration acceleration RMS value of the vehicle gradually increases.

As listed in Table 2, for the case with bridge deck roughness of level A, the weighted vibration acceleration RMS value of vehicles is 0.14 m/s^2, being less than 0.315 m/s^2, and the vehicle is not uncomfortable. For the case with bridge deck roughness of level B, the weighted vibration acceleration RMS value of vehicles is 0.97 m/s^2, falling in the range of 0.5~l m/s^2, and the vehicle is a bit uncomfortable. For the cases with bridge deck roughness of levels C and D,

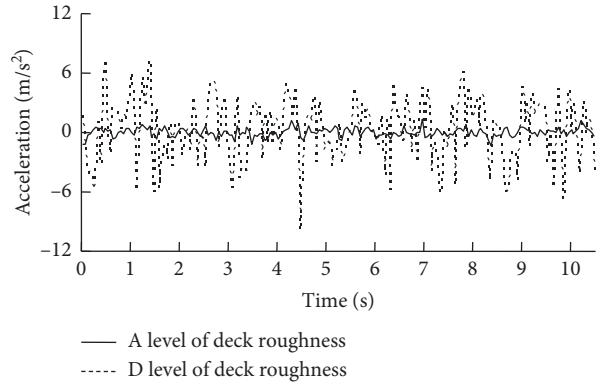

Figure 8: The time-history curves of vertical vibration accelerations of the vehicle body.

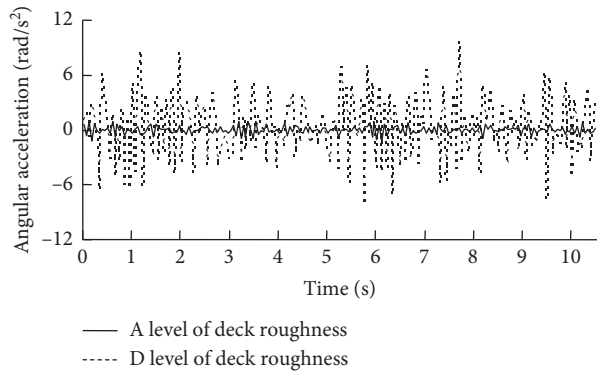

Figure 9: The time-history curves of pitching vibration accelerations of the vehicle body.

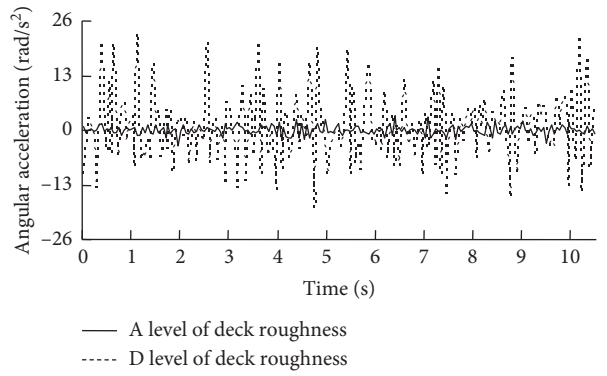

Figure 10: The time-history curves of rolling vibration accelerations of the vehicle body.

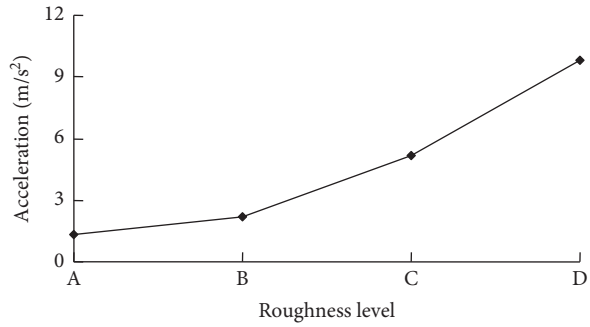

Figure 11: The variation curve of peak values of vertical vibration accelerations of the vehicle body.

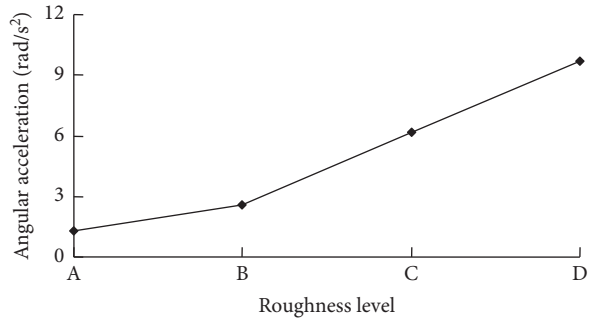

Figure 12: The variation curve of peak values of pitching vibration accelerations of the vehicle body.

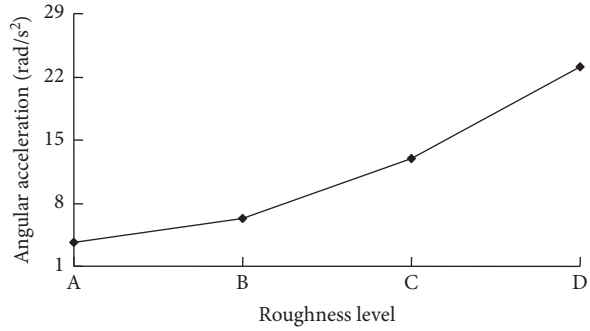

Figure 13: The variation curve of peak values of rolling vibration accelerations of the vehicle body.

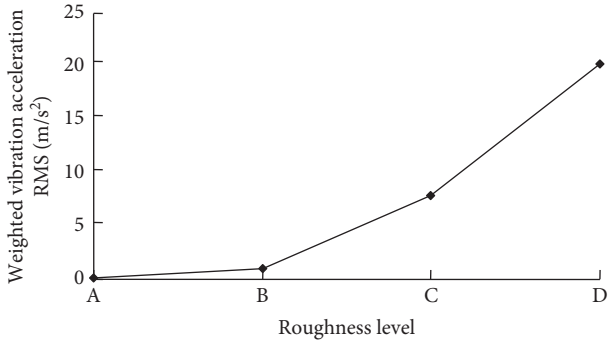

Figure 14: The variation curve of weighted vibration acceleration RMS value of the vehicle body.

the weighted vibration acceleration RMS values of vehicles are, respectively, 8.07 m/s^2 and 20.73 m/s^2, being much larger than 2 m/s^2, and the vehicle is extremely uncomfortable.

4.2. Influence of Vehicle Speed on Vehicle Comfort

4.2.1. Analysis of Vibration Acceleration of Vehicle Body. The time-history curves of vertical, pitching, and rolling vibration accelerations for the cases with vehicle speeds of 5 m/s and 40 m/s are, respectively, shown in Figures 15–17. It can be seen from the figures that, for the case with a vehicle speed of 40 m/s, the amplitudes of vertical, pitching, and rolling vibration accelerations are much larger than those for the case with a vehicle speed of 5 m/s.

The variation curves of peak values of vertical, pitching, and rolling vibration accelerations of the vehicle body with the variation of vehicle speed are, respectively, shown in Figures 18–20. As can be seen from the figures, with the increment of vehicle speed, the peak acceleration values of vertical, pitching, and rolling vibrations gradually increase. When the speed is 5 m/s, the acceleration peak values of vertical, pitching, and rolling vibrations of the vehicle body are, respectively, 0.65 m/s^2, 0.49 rad/s^2, and 1.45 rad/s^2. When the vehicle speed is 40 m/s, they are, respectively, 4.09 m/s^2, 5.95 rad/s^2 and 11.20 rad/s^2 and are increased by 3.44 m/s^2, 5.46 rad/s^2, and 9.75 rad/s^2. Therefore, the vehicle speed has an important influence on the dynamic responses of the vehicle body; especially, the rolling vibration acceleration is most sensitive to its influence.

4.2.2. Vehicle Ride Comfort Analysis. The curve of weighted vibration acceleration RMS value with the change of vehicle speed is shown in Figure 21. It can be seen from the figure that, with the increment of vehicle speed, the RMS value of weighted vibration acceleration slowly increases at the beginning and rapidly increases with the continuous increment of vehicle speed and finally approximately changes linearly.

As shown in Table 3, when the vehicle speed is 5 m/s and 10 m/s, the RMS values of vehicle weighted vibration acceleration are, respectively, 0.02 m/s^2 and 0.10 m/s^2, being less than 0.315 m/s^2, and the vehicle is not uncomfortable. When the vehicle speed is 20 m/s, the RMS value of vehicle weighted vibration acceleration is 1.15 m/s^2, falling in the range of 0.8~1.6 m/s^2, and the vehicle is uncomfortable. When the vehicle speed is 30 m/s and 40 m/s, the RMS values of vehicle weighted vibration acceleration are, respectively, 2.98 m/s^2 and 5.80 m/s^2, being larger than 2 m/s^2, and the vehicle is extremely uncomfortable.

Hu and Wang research conclusion is that the vertical acceleration of vehicles is related to the speed, and the faster the speed, the greater the amplitude of the vertical acceleration [15]. Han and Chen research results show that the RMS of vehicle vertical, pitching, and rolling acceleration augments with the increment of vehicle speed. The research conclusion of this paper is that the vehicle dynamic

Table 2: The effects of road roughness on the vehicle ride comfort.

Level of road roughness	Weighted vibration acceleration RMS value of vehicle (m/s^2)	Comfort level
A	0.1423	Not uncomfortable
B	0.9661	A little uncomfortable
C	8.0670	Extremely uncomfortable
D	20.7305	Extremely uncomfortable

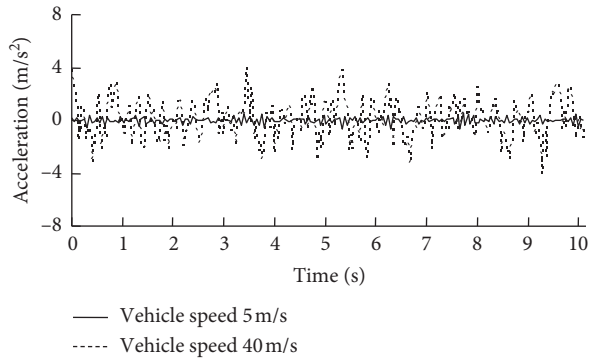

Figure 15: The time-history curves of vertical vibration accelerations of the vehicle body.

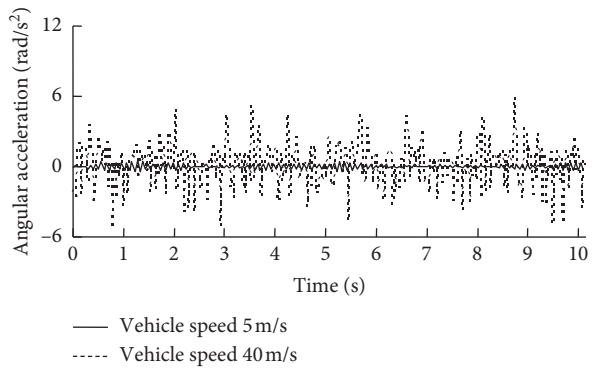

Figure 16: The time-history curves of pitching vibration accelerations of the vehicle body.

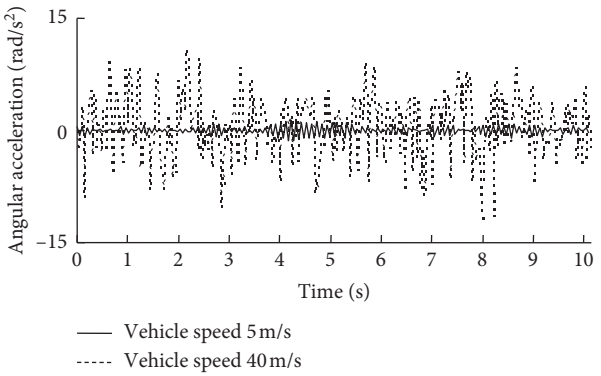

Figure 17: The time-history curves of rolling vibration accelerations of the vehicle body.

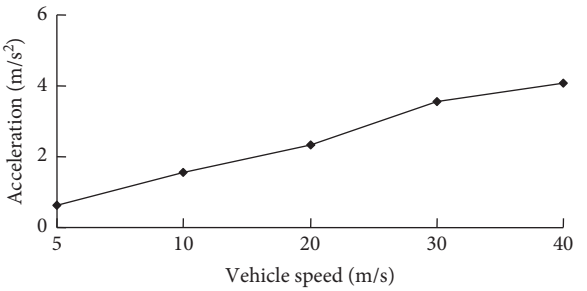

Figure 18: The variation curve of peak values of vertical vibration accelerations of the vehicle body.

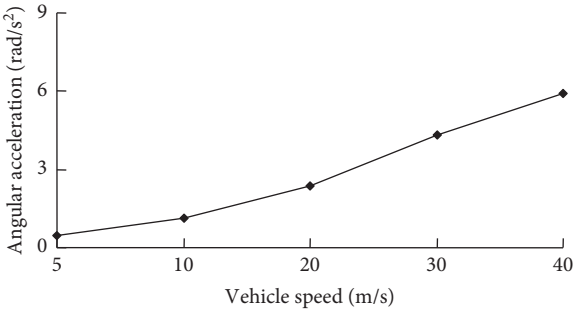

Figure 19: The variation curve of peak values of pitching vibration accelerations of the vehicle body.

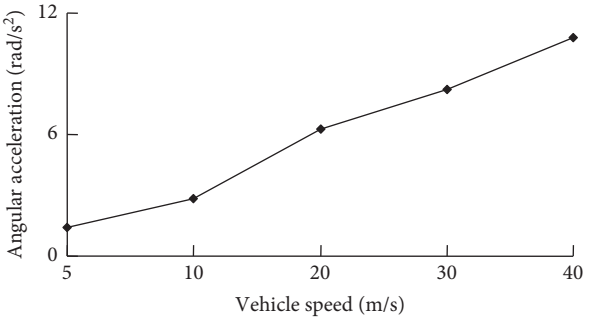

Figure 20: The variation curve of peak values of rolling vibration accelerations of the vehicle body.

responses increase with the increment of vehicle speed, and the vehicle comfort becomes worse. By comparison, the above conclusions are consistent and universal [17].

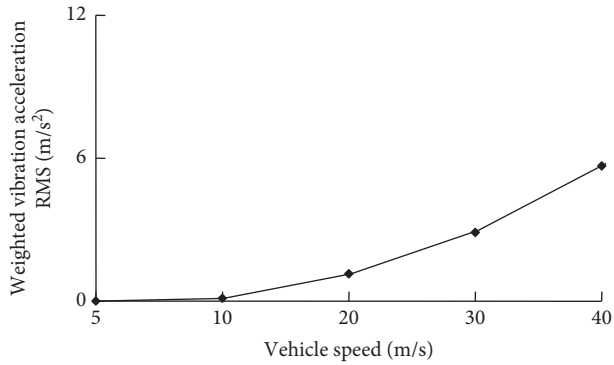

Figure 21: The variation curve of weighted vibration acceleration root mean square (RMS) value of the vehicle body.

Table 3: The effects of vehicle speed on the vehicle ride comfort.

Vehicle speed	Weighted vibration acceleration RMS value of vehicle (m/s^2)	Comfort level
5	0.0176	Not uncomfortable
10	0.1015	Not uncomfortable
20	1.1508	Uncomfortable
30	2.9787	Extremely uncomfortable
40	5.7984	Extremely uncomfortable

4.3. Influence of Vehicle Weight on Vehicle Comfort

4.3.1. Analysis of Vibration Acceleration of Vehicle Body. The time-history curves of vertical, pitching, and rolling vibration accelerations when the weight of the vehicle is 10 t and 40 t are, respectively, shown in Figures 22–24. According to the figures, when the vehicle weight is 40 t, the amplitudes of vertical, pitching, and rolling vibrations acceleration are much lower than those when the vehicle weight is 10 t.

The peak acceleration value curves of vertical, pitching, and rolling vibrations of the vehicle body are, respectively, shown in Figures 25–27. As can be seen from the figures, with the increment of vehicle weight, the peak accelerations of vertical, pitching, and rolling vibrations gradually decrease. When the vehicle weight is 10 t, the peak acceleration values of vertical, pitching, and rolling vibrations are, respectively, 5.74 m/s^2, 4.42 rad/s^2, and 6.95 rad/s^2. When the vehicle weight is 40 t, they are, respectively, 2.01 m/s^2, 2.24 rad/s^2, and 5.66 rad/s^2 and are, respectively, reduced by 3.73 m/s^2, 1.36 rad/s^2, and 1.29 rad/s^2. Therefore, vehicle weight has an important influence on vehicle dynamic responses.

4.3.2. Vehicle Ride Comfort Analysis. The variation curve of weighted vibration acceleration RMS value of the vehicle body with the change of vehicle weight is shown in Figure 28. As can be seen from the figure, with the increment of vehicle weight, the weighted vibration acceleration RMS value of the vehicle decreases rapidly. With the continuous increment of vehicle weight, the weighted vibration acceleration RMS value of the vehicle gradually and slowly decreases.

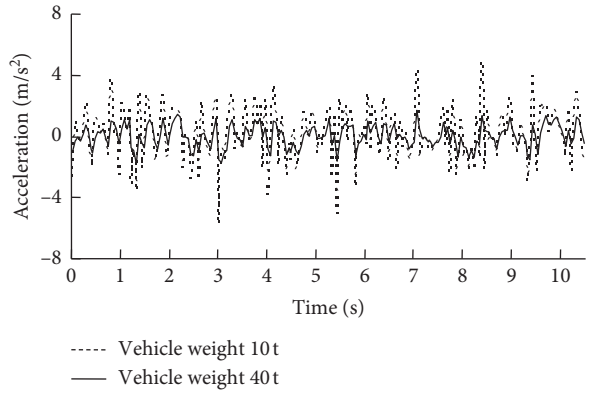

Figure 22: The time-history curves of vertical vibration accelerations of the vehicle body.

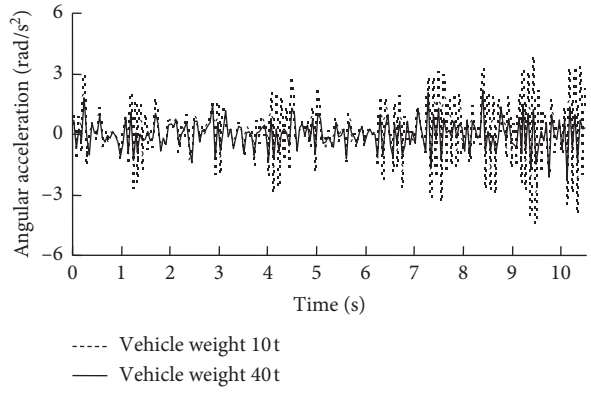

Figure 23: The time-history curves of pitching vibration accelerations of the vehicle body.

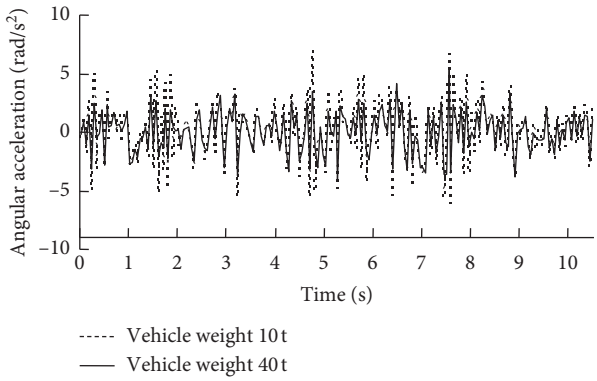

Figure 24: The time-history curves of rolling vibration accelerations of the vehicle body.

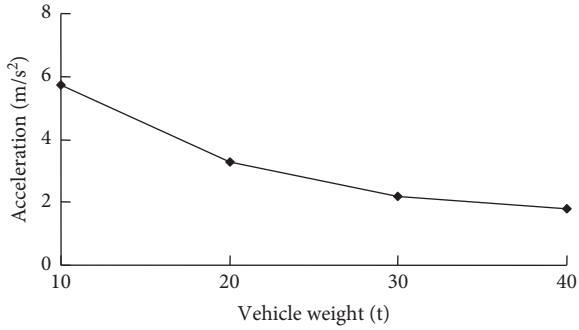

Figure 25: The variation curve of peak values of vertical vibration accelerations of the vehicle body.

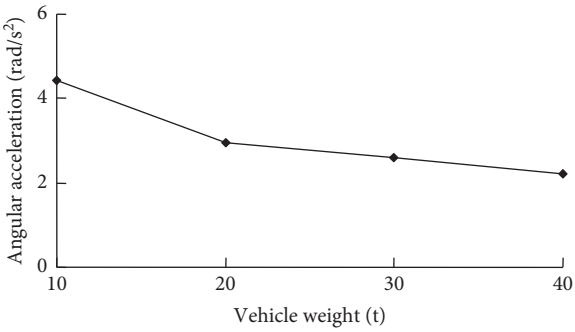

Figure 26: The variation curve of peak values of pitching vibration accelerations of the vehicle body.

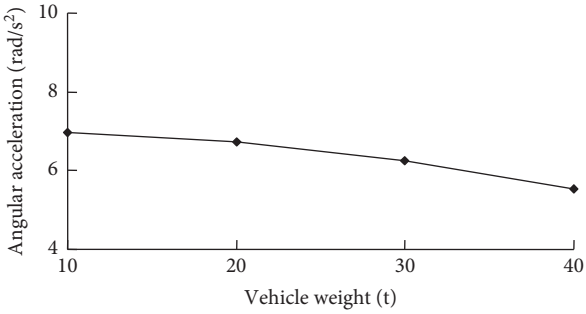

Figure 27: The variation curve of peak values of rolling vibration accelerations of the vehicle body.

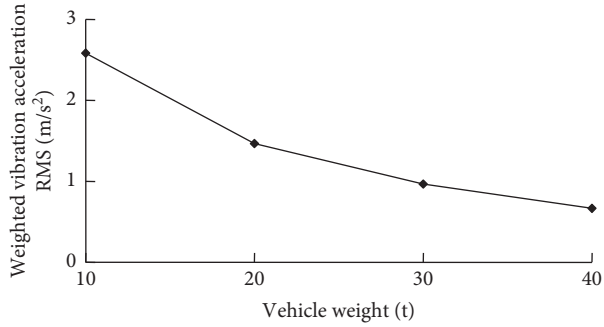

Figure 28: The variation curve of weighted vibration acceleration RMS value of the vehicle body.

As listed in Table 4, when the vehicle weight is 10 t, the weighted vibration acceleration RMS value of the vehicle body is 2.58 m/s^2, being greater than 2 m/s^2, and the vehicle is extremely uncomfortable. When the vehicle weight is 20 t, the weighted vibration acceleration RMS value of the vehicle body is 1.47 m/s^2, falling in the range of 1.25~2.5 m/s^2, and the vehicle is very uncomfortable. When the vehicle weight is 30 t, the weighted vibration acceleration RMS value of the vehicle body is 0.97 m/s^2, falling in the range of 0.8~1.6 m/s^2, and the vehicle is uncomfortable. When the vehicle weight is 40 t, the weighted vibration acceleration RMS value of the vehicle body is 0.66 m/s^2, falling in the range of 0.5~1 m/s^2, and the vehicle is somewhat uncomfortable. It can be seen

Table 4: The effects of vehicle gravity on the vehicle ride comfort.

Vehicle gravity (t)	Weighted vibration acceleration RMS value of vehicle (m/s^2)	Comfort level
10	2.5779	Extremely uncomfortable
20	1.4679	Very uncomfortable
30	0.9661	Uncomfortable
40	0.6613	Somewhat uncomfortable

that vehicle comfort is getting better and better with the increment of vehicle weight. The reason is that vehicle tends to stabilize as the weight of the vehicle increases and the vibration is reduced.

The Hu et al. research results show that the smaller the axle weight is, the larger the RMS value of vertical acceleration on the upper part of the vehicle is and the worse the ride comfort is. The research conclusion of this paper is that the vehicle dynamic responses decrease and the vehicle comfort becomes better with the increment of vehicle weight [23]. By comparison, the above conclusions are consistent and universal.

5. Implications

Taking the cable-stayed bridge with a span of 550 m as the background, setting up a six-axle freight model, and considering the influence of the vertical acceleration, pitching acceleration, and roll acceleration, we propose a comprehensive vehicle ride comfort judgment method in this paper and use the method to analyze the effects of road surface, vehicle speed, and vehicle weight on vehicle ride comfort.

The roughness of the bridge deck surface will bring discomfort to passengers, which is caused by the dynamic interaction between vehicle and bridge. With the increment of the amplitude of the bridge deck roughness, the vehicle-bridge interaction will increase accordingly. Soliman [29] also conducted the same research. He set up two typical roads, small road, and sidewalk, with roughness coefficients of 5×10^{-6} and 1×10^{-5}, respectively. The study concluded that, with the decrease of roughness coefficient, the vertical vibration acceleration of the vehicle body would decrease accordingly. The conclusion is consistent and universal, which proves the reliability of the method presented in this paper. In addition, compared with previous studies, the analysis in this paper is more comprehensive. On the one hand, the vibration of three directions of freedom, namely, vertical acceleration, pitch acceleration, and roll acceleration, is simulated in this paper. On the other hand, 4 pavement grades are taken and the parameters are adjusted to make the vibration characteristics more significant in this paper, which further lays a foundation for accurate vibration control in pavement roughness. In practical engineering, special attention should be paid to the maintenance of the bridge deck in the late operation of the bridge to reduce the impact of bridge deck conditions on vehicle-induced bridge vibration.

Under a certain roughness bridge deck, the increase of speed will reduce the comfort of vehicles. This is because, with the increase of speed, the roughness of bridge deck will lead to the increase of impulse of vehicle load, which will lead to the gradual increase of vibration responses of vehicles and bridge deck. Therefore, in the actual situation, attention should be paid to reduce the driving speed in the uneven section of bridge deck to reduce its impact. Chen et al. [30] set the vehicle speed from 40 km/h to150 km/h to explore the influences of vehicle speed on vehicle comfort and found that, with the increase of vehicle speed, the body's gravitational acceleration also increases and the vehicle comfort decreases. This is consistent and universal with the research results in this paper, which proves the accuracy of the method in this paper. In addition, the speed taken in this paper ranges from 5 km/h to 40 km/h, that is, the relationship between speed and vehicle comfort at low speed, which complements the theoretical research on the effect of speed on vehicle comfort.

The increase of vehicle weight can make vehicles more stable and increase the comfort of passengers and drivers. This is because, with the increase of vehicle body weight and increase of inertia of the vehicle body, the movement of the vehicle body state is not easy to change; in addition, in real life, with vehicle body weight increase, the energy that vehicle body absorbs increases, and then the energy accepted by the human body is less. Yao [31] set three vehicle mass conditions of 6451 kg, 12902 kg, and 22451 kg for numerical simulation, proved that the maximum vertical acceleration response of the vehicle body decreases with the increase of vehicle load, which is consistent and universal with the research results in this paper, and proved the accuracy of the method in this paper. Moreover, the research interval of this paper is 10 t–40 t, which further improves the research theory of vehicle weight on vehicle comfort and lays a foundation for further accurate vibration control in vehicle weight.

In this paper, the vehicle-bridge model was established by ANSYS APDL, and iso2631-1-1997 evaluation standard was used to analyze the vertical acceleration, pitch acceleration, and roll acceleration of vehicles under different bridge deck grades, vehicle speed, and vehicle weight, so as to study the influence of bridge deck roughness, vehicle speed, and vehicle weight on vehicle body comfort. It is concluded that bridge deck roughness, vehicle speed, and vehicle weight have a significant influence on vehicle comfort.

Through the study in this paper, the vibration characteristics are more significant, which further lays a good foundation for the study of vehicle comfort in three aspects: deck roughness, vehicle speed, and vehicle weight. The practical significance of this paper is to study the influence of deck roughness, vehicle speed, and vehicle weight on vehicle comfort and to provide reasonable advice for the design of bridge deck, vehicle speed, and vehicle weight control.

6. Conclusion

In this paper, the vehicle-bridge model was established by ANSYS APDL, and iso2631-1-1997 evaluation standard was used to analyze the vertical acceleration, pitch acceleration, and roll acceleration of vehicles under different bridge deck roughness, vehicle speed, and vehicle weight, so as to study the influence of bridge deck roughness, vehicle speed, and vehicle weight on vehicle body comfort. It is concluded that bridge deck roughness, vehicle speed, and vehicle weight have a significant influence on vehicle comfort. With the deterioration of irregular shape of the bridge deck, the peak acceleration of vertical vibration, pitch vibration, and roll vibration increases gradually, and the ride comfort of vehicles becomes worse and worse. With the increase of vehicle speed, the peak values of vertical vibration, pitch vibration, and rolling vibration increase gradually. The RMS of the weighted vibration acceleration of the vehicle increases slowly first and then rapidly, and finally, it changes approximately linearly and the vehicle comfort becomes worse and worse. With the increase of vehicle weight, the peak values of vertical vibration, pitch vibration, and rolling vibration decrease gradually. The RMS of the weighted vibration acceleration of the vehicle decreases rapidly at the beginning. As the weight of the vehicle increases, the reduction rate gradually flattens out. Vehicle ride is getting better and better.

Through the study in this paper, the vibration characteristics are more significant, which further lays a good foundation for the study of vehicle comfort in three aspects: deck roughness, speed, and vehicle weight. The practical significance of this paper is to study the influence of deck roughness, vehicle speed, and vehicle weight on vehicle comfort and to provide reasonable advice for the design of bridge deck, vehicle speed, and vehicle weight control.

Data Availability

The data used to support the findings of this study are available from the corresponding author upon request.

Conflicts of Interest

The authors declare no conflicts of interest.

Acknowledgments

The authors gratefully acknowledge the financial support from the National Natural Science Foundation of China (Foundation no. 50878198).

References

[1] J. Oliva, J. M. Goicolea, P. Antolín, and M. Á. Astiz, "Relevance of a complete road surface description in vehicle-bridge interaction dynamics," *Engineering Structures*, vol. 56, pp. 466–476, 2013.

[2] J. Y. Zheng, Y. H. Chen, and J. P. Wang, "Finite element analysis on coupled vehicle-bridge vibration based on the sprung mass model," *Applied Mechanics and Materials*, vol. 687–691, pp. 249–254, 2014.

[3] J.-D. Yau and L. Frýba, "A quasi-vehicle/bridge interaction model for high speed railways," *Journal of Mechanics*, vol. 31, no. 2, pp. 217–225, 2015.

[4] S. Vishwas, "Dynamic analysis of rigid pavement with vehicle-pavement interaction," *Journal of Pavement Engineering*, vol. 10, no. 1, pp. 63–72, 2009.

[5] Kwon, M. Lee, and Kim, "Dynamic interaction analysis of urban transit maglev vehicle and guideway suspension bridge subjected to gusty wind," *Engineering Structures*, vol. 30, no. 12, pp. 445–456, 2008.

[6] A. T. Saeed and Z. Xiang, "Dynamic analysis of coupling vehicle-bridge system using finite prism method," *International Journal of Engineering and Technology*, vol. 9, no. 5, pp. 359–365, 2017.

[7] M. A. Koç and İ. Esen, "Modelling and analysis of vehicle-structure-road coupled interaction considering structural flexibility, vehicle parameters and road roughness," *Journal of Mechanical Science and Technology*, vol. 31, no. 5, pp. 2057–2074, 2017.

[8] S. Zhou, G. Song, R. Wang, Z. Ren, and B. Wen, "Nonlinear dynamic analysis for coupled vehicle-bridge vibration system on nonlinear foundation," *Mechanical Systems and Signal Processing*, vol. 87, pp. 259–278, 2017.

[9] S. Q. Wu and S. S. Law, "Dynamic analysis of bridge-vehicle system with uncertainties based on the finite element model," *Probabilistic Engineering Mechanics*, vol. 25, no. 4, pp. 425–432, 2010.

[10] D. Provornaya and S. Glushkov, "Vehicle-bridge interaction system," in *Proceedings of the MATEC Web of Conferences*, vol. 239, Article ID 05004, Leeds, UK, July 2018.

[11] M. Ouchenane, "Study of the vibratory behavior of the bridge under the passage of mobile loads convoys: comparative study between uni-dimensional and three-dimensional modeling," *Civil Engineering Journal*, vol. 4, no. 5, p. 926, 2018.

[12] H. Moghin and H. R. Ronagh, "Development of a numerical model for bridge-vehicle interaction and human response to traffic-induced vibration," *Engineering Structures*, vol. 30, no. 12, pp. 3808–3819, 2008.

[13] J. A. Zakeri, M. M. Feizi, M. Shadfar, and M. Naeimi, "Sensitivity analysis on dynamic response of railway vehicle and ride index over curved bridges," *Proceedings of the Institution of Mechanical Engineers, Part K: Journal of Multi-Body Dynamics*, vol. 231, no. 1, pp. 266–277, 2017.

[14] C. Mizrak and I. Esen, "The optimisation of rail vehicle bogie parameters with the fuzzy logic method in order to improve passenger comfort during passage over bridges," *International Journal of Heavy Vehicle Systems*, vol. 24, no. 2, pp. 113–139, 2017.

[15] Z. Hu and H. Wang, "Analysis of comfort properties for high-speed vehicle moving over bridge," *Journal of Vibration and Shock*, vol. 21, no. 4, pp. 104-105, 2002.

[16] Y. L. Xu and W. H. Guo, "Effects of bridge motion and crosswind on ride comfort of road vehicles," *Journal of Wind Engineering and Industrial Aerodynamics*, vol. 92, no. 7-8, pp. 641–662, 2004.

[17] W. Han and A. Chen, "Ride comfort assessment of vehicles running on long-span bridge under crosswind," *China Journal of Highway and Transport*, vol. 21, no. 2, pp. 54–60, 2008.

[18] W. Han and A. Chen, "Effects of crosswind and bridge motion on ride comfort of road vehicles," *China Civil Engineering Journal*, vol. 41, no. 4, pp. 55–60, 2008.

[19] Y.-W. Zhang, Y. Zhao, Y.-H. Zhang, J.-H. Lin, and X.-W. He, "Riding comfort optimization of railway trains based on pseudo-excitation method and symplectic method," *Journal ff Sound and Vibration*, vol. 332, no. 21, pp. 5255–5270, 2013.

[20] W. Wu, C. Shu, Z. Yang, Y. Wu, and X. Wang, "Vibration control and comfort evaluation about Qijia yellow river bridge," *Journal of Highway and Transportation Research and Development*, vol. 26, no. 2, pp. 42–46, 2009.

[21] Q. F. Gao, Z. L. Wang, C. Chen, and B. Q. Guo, "Comfort analysis of large-span continuous girder bridges to moving vehicular loads," *Key Engineering Materials*, vol. 619, pp. 61–70, 2014.

[22] M. Bouazara and M. J. Richard, "An optimization method designed to improve 3-D vehicle comfort and road holding capability through the use of active and semi-active suspensions," *European Journal of Mechanics-A/Solids*, vol. 20, no. 3, pp. 509–520, 2001.

[23] T. Hu, G. Yin, and M. Sun, "Model based research of dynamic performance of shaft-bearing system in high-speed field," *Shock and Vibration*, vol. 2014, Article ID 478270, 12 pages, 2014.

[24] D. Hubbell and G. Paul, "Frequency domain analysis of train–guideway interaction dynamics," *Journal of Structural Engineering*, vol. 144, no. 8, Article ID 04018100, 2018.

[25] Wu-sheng, *The Analysis on the Security and Vehicle Comfortableness of Vehicle-Bridge Coupling Vibration System of Highway Cable-stayed Bridge with Long-Span*, Zhengzhou University, Zhengzhou, China, 2016.

[26] ISO2631-1, *Mechanical Vibration and Shock-Evaluation of Human Exposure to Whole-Body Vibration-Part 1: General Requirements*, International Organization for Standardization, Geneva, Switzerland, 1997.

[27] G. Loprencipe, P. Zoccali, and G. Cantisani, "Effects of vehicular speed on the assessment of pavement road roughness," *Applied Sciences*, vol. 9, no. 9, p. 1783, 2019.

[28] G. Loprencipe and P. Zoccali, "Ride quality due to road surface irregularities: comparison of different methods applied on a set of real road profiles," *Coatings*, vol. 7, no. 59, p. 16, 2017.

[29] A. M. A. Soliman, "Effect of road roughness on the vehicle ride comfort and rolling resistance," in *Proceedings of the SAE 2006 World Congress*, Detroit, Michigan, April 2006.

[30] S. Chen, D. Wang, A. Zuo, Z. Chen, W. Li, and J. Zan, "Vehicle ride comfort analysis and optimization using design of experiment," in *Proceedings of the 2010 Second International Conference on Intelligent Human-Machine Systems and Cybernetics*, Nanjing, China, August 2010.

[31] C. Yao, *Coupling Vibration Analysis of Highway Vehicle-Bridge Considering the Influence of Bridge Deck Irregularity*, Central South University, Changsha, China, 2011.